# Continuous Synthesis of Oxymethylene Ether Fuels from Dimethyl Ether in a Heterogeneously Catalyzed Liquid Phase Process

**Marius Drexler, Philipp Haltenort, Ulrich Arnold\*, and Jörg Sauer**

Supporting Information available online

***Dedicated to Prof. Dr. Thomas Hirth on the occasion of his 60th birthday***

Oxymethylene ethers (OME) are an attractive alternative to fossil diesel fuel due to strongly reduced harmful emissions. An anhydrous, liquid phase production process based on dimethyl ether (DME) has been elaborated, which offers high selectivity and economic advantages. A catalyst screening for the reaction of DME with trioxane has been carried out. Highly active catalysts could be identified and further insight into the relationship between catalyst properties and catalytic performance could be gained. Furthermore, production in a continuous process could be realized, disclosing the influence of kinetics on OME formation and enabling a better understanding of the reaction mechanism.

## 1 Introduction

Oligomeric oxymethylene ethers (OME) of the type $CH_3O(CH_2O)_nCH_3$ (Fig. 1) are currently drawing considerable attention as an alternative synthetic diesel fuel [1]. Especially OME with a chain length of $n$ = 3–5 are an attractive option to substitute fossil diesel fuel due to their extensive compliance to current fuel standards [2, 3]. A particularly interesting feature of OME for fuel applications is the absence of carbon-carbon bonds in their molecular structure, resulting in a virtually soot-free combustion [4–6]. This allows to avoid the soot-$NO_x$ trade-off and therefore optimization of engine operation to minimize soot as well as $NO_x$ emissions [7–9]. The result is a very clean combustion process with strongly reduced harmful emissions while lowering complex and costly exhaust gas treatment [7, 10]. Thus, compliance to increasingly stricter emission restrictions becomes feasible [11]. OME can be applied as a pure fuel with reasonable modifications of the engine and fuel system but also as a blending component to fossil diesel fuel [12–14].
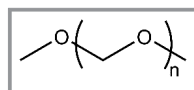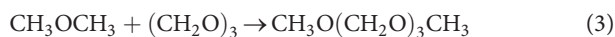
OME can be produced from methanol or its derivatives and formaldehyde (FA) sources. Employing green methanol, OME can be produced from renewable resources [15, 16], drastically reducing the carbon footprint of the synthetic fuel [17–19]. In general, the reaction is catalyzed by acids and production pathways for OME can be divided in aqueous and anhydrous routes. Anhydrous production of OME usually starts from dimethoxymethane (DMM, $OME_1$) and trioxane (TRI), which are synthesized from methanol and FA in well-established processes. While offering high selectivity, this pathway employs costly starting materials and is therefore hardly feasible for the production of synthetic fuel. Current research efforts aim for the direct production of OME from methanol and aqueous FA solutions to avoid such costly reactants [20, 21]. However, this leads to complex purification processes for the product mixtures since numerous by-products are formed, e.g., hemiformals, if water is present during OME synthesis.

**Figure 1.** Molecular structure of OME.

Marius Drexler, Philipp Haltenort, Dr. Ulrich Arnold, Prof. Dr.-Ing. Jörg Sauer
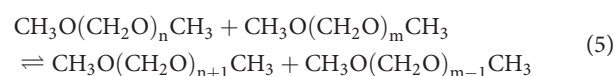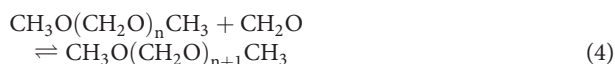ulrich.arnold@kit.edu
Karlsruhe Institute of Technology (KIT), Institute of Catalysis Research and Technology (IKFT), Hermann-von-Helmholtz-Platz 1, 76344 Eggenstein-Leopoldshafen, Germany.

These need to be separated and water needs to be removed as well [22–25]. In view of these obstacles, a liquid phase process for the production of OME from dimethyl ether (DME, $OME_0$) and dry FA has been proposed. This strategy benefits from the advantages of an anhydrous process while avoiding costly reactants such as DMM [26]. Though being a promising option, literature on this pathway is scarce. As monomeric dry FA is extremely reactive, stable derivatives such as TRI, the cyclic trimer of FA, can be used as model substances. For an efficient production of synthetic fuel, usage of such costly substitutes needs to be avoided and in the long run, OME should be produced directly from dry FA in an integrated process. Employing TRI as a source of dry FA, previous studies showed that zeolite H-BEA-25 is an effective catalyst for this reaction while ion exchange resins did not show appreciable catalytic activity [27]. Additionally, kinetic control of the reaction to influence selectivity and the product spectrum has been demonstrated [27]. The reaction proceeds in two stages and the proposed network is illustrated in Fig. 2.

In the first stage, OME formation occurs by generation of monomeric FA from TRI decomposition (Eq. (1)) and subsequent FA incorporation into DME to give $OME_1$ (Eq. (2)). Alternatively, $OME_3$ formation by direct incorporation of TRI into DME has been discussed (Eq. (3)) [27].

$$(CH_2O)_3 \rightarrow 3\ CH_2O \tag{1}$$

$$CH_3OCH_3 + CH_2O \rightarrow CH_3O(CH_2O)_1CH_3 \tag{2}$$

$$CH_3OCH_3 + (CH_2O)_3 \rightarrow CH_3O(CH_2O)_3CH_3 \tag{3}$$

In the second stage, OME chain length adjusts either by reaction with FA (Eq. (4)) [28] or by transacetalization reactions, i.e., intermolecular exchange of FA units (Eq. (5)) [29]. Finally, a Flory-Schulz product distribution is adopted [30–32].

$$CH_3O(CH_2O)_nCH_3 + CH_2O \rightleftharpoons CH_3O(CH_2O)_{n+1}CH_3 \tag{4}$$

$$CH_3O(CH_2O)_nCH_3 + CH_3O(CH_2O)_mCH_3 \rightleftharpoons CH_3O(CH_2O)_{n+1}CH_3 + CH_3O(CH_2O)_{m-1}CH_3 \tag{5}$$

The main byproduct methyl formate (MeFo), which is currently investigated as a substitute for fossil gasoline [33, 34], is formed from two molecules of FA in a Tishchenko reaction according to Eq. (6) [35].
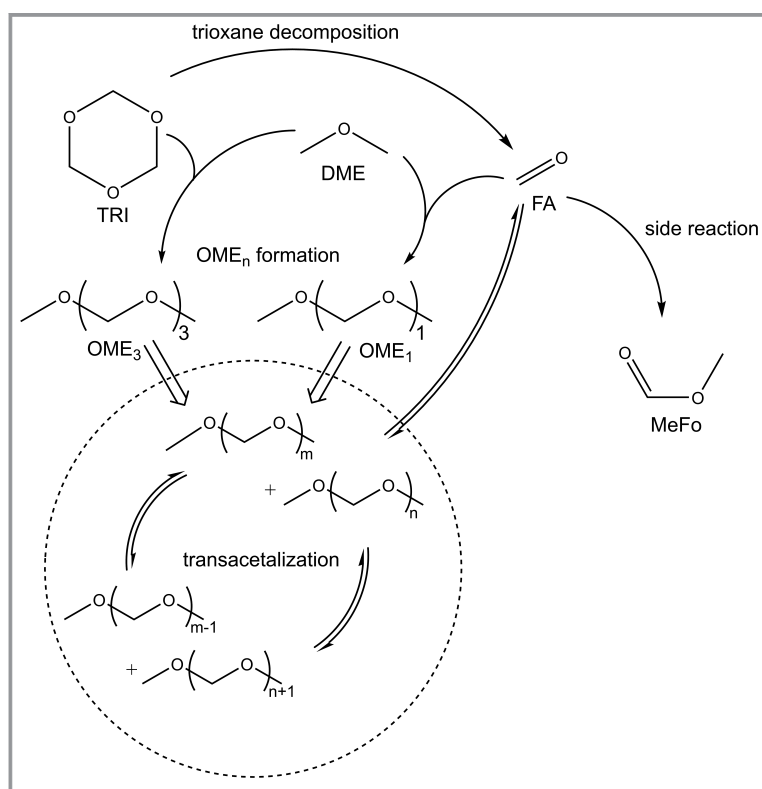
$$2\ CH_2O \rightarrow HCOOCH_3 \tag{6}$$

While formation of MeFo is the only side reaction under strictly anhydrous conditions, traces of water or methanol in the starting materials might lead to the occurrence of other byproducts known from alternative OME synthesis processes, such as hemiformals, methylene glycols or formic acid [20, 36].

In the present study, suitability of various heterogeneous catalysts for the production of OME from DME and TRI as a source of dry FA has been investigated. Montmorillonite K10, an inexpensive and eco-friendly clay material [37, 38], has been employed. Due to its layered structure the material offers ion-exchange properties, allowing for facile modification by intercalation of various cations. Using ion exchange techniques known from literature, various K10 catalysts have been prepared. Previous work indicated activity of such catalysts in the context of OME formation from $OME_1$ and TRI as well as paraformaldehyde and alcohols [39, 40]. Additionally, various zeolites have been tested for OME synthesis from $OME_1$ and TRI [41–44]. Since zeolites are very versatile materials in terms of adjustable acidity as well as morphologic properties while also being very stable and recyclable, they represent a promising and cost-efficient class of catalysts for the production of synthetic fuels [41, 45]. For OME synthesis from DME and TRI catalytic activity of H-BEA-25



**Figure 2.** Reaction network for OME synthesis from DME and TRI (all reactions are catalyzed by acids, reactions affecting OME chain length are framed with a dashed circle).

has been reported in previous work [27]. Thus, catalysts tested in this study comprise zeolites with the frameworks BEA, MFI and FAU with different $SiO_2/Al_2O_3$ ratios and with H-BEA-25 as the state-of-the-art reference. Furthermore, continuous production of OME from DME in a liquid phase process has been carried out in a laboratory scale plant. Thus, previous studies based on batch experiments [27] have been extended and kinetic control of the reaction by variation of the weight hourly space velocity (WHSV) has been investigated in detail.

## 2 Experimental

### 2.1 Materials

DME (99.9 %) was obtained from basi Schöberl GmbH & Co. KG. TRI (> 99.9 %) and n-dodecane (≥ 99.9 %) were purchased from Sigma Aldrich. The montmorillonite K10 clay catalyst has been obtained from Fluka. Ion exchanged K10 materials have been prepared according to methods described in literature [46–48]. 5 g of the K10 powder were suspended in 200 mL of a 0.5 M aqueous solution containing the desired cation and stirred at room temperature for 24 h. After separation by centrifugation, the powder was washed with deionized water. The product was dried and ground in a mortar. Using this procedure, materials containing iron, aluminum and tin have been prepared employing $FeCl_3$ (≥ 98 %, Merck), $Al(NO_3)_3 \cdot 9H_2O$ (≥ 98 %,

Fluka) and $SnCl_4$ (anhydrous, 98 %, Alfa Aesar). Acid treatment of the material has been carried out according to the procedures of Reddy et al. [47]. Hydrochloric acid (37 %, Merck) has been used and a concentration of 0.5 M has been adjusted. Additionally, a sulfonated K10 catalyst was prepared according to the procedures of Shinri et al. [49] employing chlorosulfonic acid (≥ 98 %, Sigma Aldrich) and chlorofom (anhydrous, ≥ 99 %, Sigma Aldrich). After treatment, the catalyst was washed with methanol (anhydrous, 99.8 %, Sigma Aldrich), dried and ground in a mortar.

Samples of commercial zeolite powders were provided by Zeolyst International. Additionally, SAPO-34 was purchased from ACS Material. All catalysts as well as some basic information provided by the manufacturers are listed in Tab. 1. Zeolites BEA-25 and ZSM-5-80 were provided as extrudates by Zeolyst International and used in the continuous experiments. All zeolites were used in H form and calcined at 500 °C for 5 h in static air. All employed catalysts have been dried at 110 °C and 10 mbar over night prior to use since inhibition of catalytic activity by water has been proven to be decisive regarding OME formation [36, 50].

### 2.2 Experimental Procedure

Screening experiments in batch mode have been carried out employing stainless-steel autoclaves (100 mL internal volume). The reactant mixtures contained TRI and DME in a molar ratio of $n_{TRI}/n_{DME} = 0.25$ adding up to 20 g and were

**Table 1.** Zeolite catalysts used for the screening experiments.

| Catalyst | Trade name | Framework type | $SiO_2/Al_2O_3$ molar ratio [–][a] | Surface area [$m^2g^{-1}$][a] | Pore diameter [Å] [51] |
|---|---|---|---|---|---|
| H-BEA-25 | CP814E* | *BEA | 25 | 680 | 6.6×6.7; 5.6×5.6 |
| H-BEA-38 | CP814C* | | 38 | 710 | |
| H-BEA-300 | CP811C-300 | | 300 | 620 | |
| H-ZSM-5-30 | CBV3024E | MFI | 30 | 405 | 5.1×5.5; 5.3×5.6 |
| H-ZSM-5-50 | CBV5524G | | 50 | 425 | |
| H-ZSM-5-80 | CBV8014G | | 80 | 425 | |
| H-ZSM-5-280 | CBV28014 | | 280 | 400 | |
| H-Y-5.2 | CBV500 | FAU | 5.2 | 750 | 7.4×7.4 |
| H-Y-12 | CBV712 | | 12 | 730 | |
| H-Y-30 | CBV720 | | 30 | 780 | |
| H-Y-60 | CBV760 | | 60 | 720 | |
| H-Y-80 | CBV780 | | 80 | 780 | |
| H-ZSM-22 | ZD05039 | TON | 97.3 | 231 | 4.6×5.7 |
| H-ZSM-23 | ZD15001 | MTT | 48 | 238 | 4.5×5.2 |
| H-SAPO-34 | SAPO-34 | CHA | ≈ 0.5 | ≥ 550 | 3.8×3.8 |

a) Values provided by the manufacturer.

**Table 2.** Feed mixtures used in the screening experiments (batch mode and continuous operation).

|  | DME [wt %] | TRI [wt %] | Dodecane [wt %] | $n_{TRI}/n_{DME}$ [mol mol$^{-1}$] |
|---|---|---|---|---|
| Feed 0 | 33.3 | 16.7 | 50 | 0.25 |
| Feed 1 | 30 | 15 | 55 | 0.24 |
| Feed 2 | 60 | 30 | 10 | 0.24 |

diluted with 20 g of dodecane (Feed 0, Tab. 2). In each experiment 0.52 g of catalyst (2.6 wt %$_R$) were employed. The reaction temperature was set to 80 °C and the reaction time was 6 h. The reaction conditions have been chosen to avoid total conversion of TRI and enabling comparison of catalyst performances. According to previous work, the low temperature should result in a broad OME distribution [27], allowing for a better comparison of the different catalysts regarding selectivity to different OME chain lengths. As TRI is involved in the formation of all products, OME$_n$ and MeFo, it was chosen as the limiting component. Consequently, DME has been employed in excess, using a molar ratio $n_{TRI}/n_{DME}$ of 0.25. This ratio has been identified previously as the optimum for the production of OME$_{3-5}$ at this temperature [27]. Dodecane was dosed into the autoclaves and TRI as well as the dry catalyst powder were added using a laboratory balance (AE200, Mettler). The autoclave was sealed and DME added using a syringe pump (Model 750.1100, Sitec, Model 500D, Teledyne Isco). Subsequently, the autoclave was placed on a magnetic stirrer unit (RCT basic, IKA). Temperature and pressure were monitored using a type K thermocouple and a mechanical pressure gauge. The final pressure due to the vapor pressure of the

reactant mixture was about 12 bar for all experiments. After reaction, the autoclave was quenched using a 0 °C ice-water bath. The autoclave was depressurized, and samples of the liquid product mixtures were taken using a syringe filter (0.45 μm) to remove catalyst particles.

Continuous OME production has been carried out in a laboratory scale plant (Fig. 3). For all experiments, the reactor temperature has been set to 100 °C and two different feed mixtures (Feed 1 and Feed 2, Tab. 2) have been employed. For the continuous experiments, catalysts have been employed in the form of extrudates.

The feed mixtures (Feed 1 and Feed 2, Tab. 2) containing TRI, DME and dodecane were prepared in a stainless-steel vessel using the same equipment as for batch experiments and transferred to the plant prior to the experiment. The catalyst was employed as a fixed bed in a tubular reactor submerged in an oil bath, which was heated by a thermostat (C35P, Thermo Haake,) to ensure isothermal conditions. The reactant mixture was dosed by a gear pump (DRIP, Gather) controlled by a Coriolis mass flow meter (mini CORI-FLOW M13, Bronkhorst). Samples of the product mixture were drawn from a sampling valve located at the reactor outlet and the product stream was collected in a stainless-steel cylinder. The plant was pressurized to 60 bar using helium (≥ 99.9 %, Air Liquide) to ensure that all components remain in the liquid phase. The pressure was monitored using a pressure transmitter (S20, WIKA) and the temperature was monitored using type K thermocouples located at the reactor inlet and outlet. During the course of the experiments the flow rate of the reactants $\dot{m}_{reactant}$ and mass of catalysts $m_{catalyst}$ were varied, resulting in different *WHSV* values (Eq. (7)).
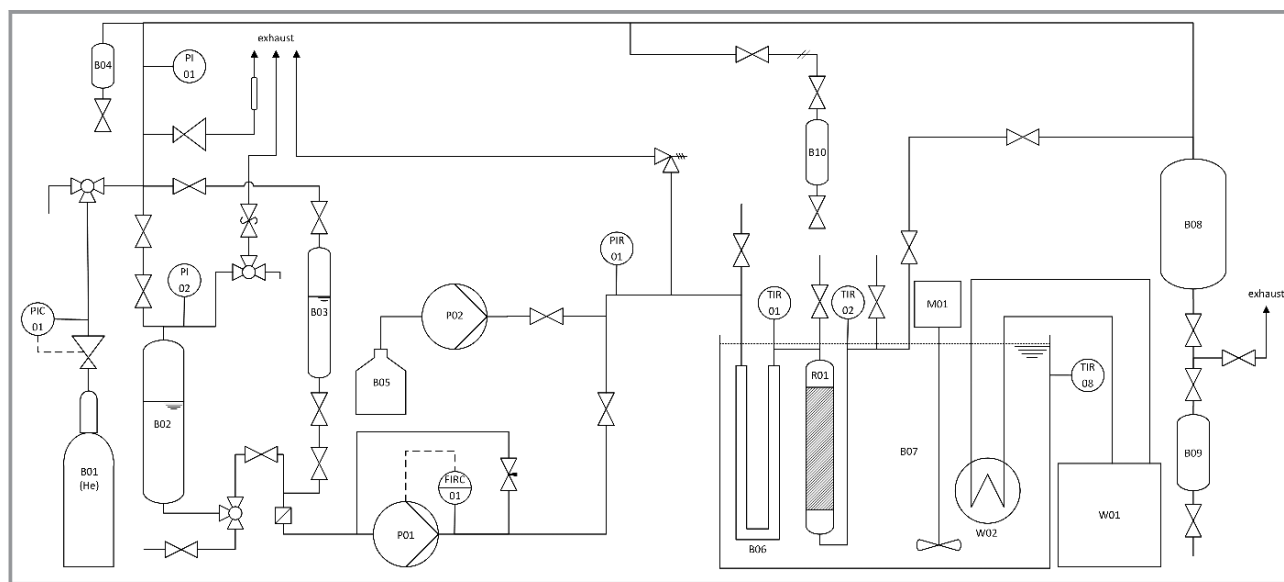


**Figure 3.** Flow diagram of the laboratory plant for continuous OME synthesis.

$$WHSV = \frac{\dot{m}_{reactant}}{m_{catalyst}} \tag{7}$$

To ensure steady-state conditions before taking samples, the reactor has been operated under constant conditions and sufficiently long intervals of 12.5 to 50 min between sampling have been chosen corresponding to at least three times of the reactor's volume of feed.

## 2.3 Analytical Methods

Compositions of the liquid samples have been analyzed employing a Hewlett Packard 6890 series FID gas chromatograph (GC), equipped with an Agilent DB-5 MS+DG column using helium as carrier gas. Response factors ($RF$) of $OME_{1-5}$, dodecane, MeFo and TRI were determined using pure compounds. The response factor of $OME_6$ was obtained by extrapolation of the values for $OME_{1-5}$. Higher OME ($OME_{6+}$) could only be detected in traces and were neglected. As DME evaporated during depressurizing, the amount remaining in the liquid phase was excluded from GC analysis. For quantification of the compounds, $n$-octane ($\geq 99\%$, Merck) was added to the samples and used as internal standard. The weight fraction of a component $\omega_i$ has been calculated according to Eq. (8).

$$\omega_i = \frac{\frac{A_i}{A_{octane}} RF_i m_{octane}}{m_{total}} \tag{8}$$

To obtain the required total mass of the liquid fraction $m_{total}$, dodecane was used as internal standard. As it remains inert during reaction, its mass remains constant, and the total mass of the liquid phase can be obtained by determining its mass fraction (Eq. (9)).

$$m_{total} = \frac{m_{dodecane}}{\omega_{dodecane}} \tag{9}$$

Conversion of TRI has been determined by calculating the mass of FA bound in the reactions products and comparing it to the mass of TRI employed (Eq. (10)).

$$X_{TRI} = \frac{m_{FA,products}}{m_{TRI}} \tag{10}$$

As DME was added in surplus the conversion of TRI was used as a measure to compare the activity of the catalysts. Since FA is involved in OME as well as MeFo formation, the selectivity of the reaction has been determined by calculating the fraction of FA fixed in OME (Eq. (11)).

$$S_{TRI,OME_{1-6}} = \frac{\sum_{i=1}^{6} m_{FA,OME_{1-6}}}{m_{FA,products}} \tag{11}$$

The product yield has been calculated according to Eq. (12). Additionally, the average chain length ($ACL$) of OME molecules has been determined as a measure for OME distribution (Eq. (13)).

$$Y_{TRI,OME_{1-6}} = X_{TRI} S_{TRI,OME_{1-6}} \tag{12}$$

$$ACL = \frac{\sum n_{FA,OME_n}}{\sum n_{OME_n}} \tag{13}$$

For the experiments regarding continuous OME production, pressurized samples have been drawn from the setup using stainless-steel sample cylinders. Total mass of the samples was determined using a laboratory balance (Type 1403MP8-1, Sartorius). Measuring standards have been added to the cylinders beforehand. If high concentrations of TRI were expected, the samples have been diluted with formaldehyde diethyl acetal ($\geq 99\%$, Merck) to avoid phase separation. By using high-pressure sample tubes, NMR analysis of the product mixtures without phase separation becomes possible. Employing a Bruker Avance 250 NMR spectrometer and toluene D8 (99.5 %D, VWR International) as solvent the weight fraction of compounds can be calculated according to Eq. (14). Toluene ($\geq 99\%$, Merck) was added to the sample cylinders as internal standard.

$$\omega_i = \frac{n_i M_i}{m_{total}} = \frac{A_i n_{toluene}}{A_{toluene}} \frac{q_{toluene}}{q_i} \frac{M_i}{m_{total}} \tag{14}$$

After depressurizing the sample cylinders the liquid product phase has been analyzed by GC using the procedure described above.

Characterization of the catalysts used in the continuous experiments was performed to gain insights into the influence of structural differences, as the properties of shaped catalysts deviate from those of catalyst powders. Nitrogen adsorption and desorption isothermes were recorded at 77.35 K using a Quantachrome Nova 2000e analyzer. Prior to analysis the samples were degassed for 20 h at 230 °C. The specific surface area was determined according to the Brunauer-Emmet-Teller method (BET) in a non-classical range of $p/p_0$ from 0.004–0.12 (Rouquerol plot). The t-plot as well as the Barret-Joyner-Halenda (BJH) method was used to determine pore area and volume.

Characterization of the nature of acidity has been carried out at Leibniz Institute for Catalysis (LIKAT Rostock) using pyridine-FTIR. A sample of 50 mg of the catalyst was compacted into a self-supporting wafer and pretreated at 400 °C for 1 h under vacuum. Pyridine desorption spectra were recorded on a Bruker Tensor 27 in steps of 50 K starting at 400 °C. Background correction was performed with a background spectrum measurement at 200 °C. Adsorption bands at 1543 cm$^{-1}$ (PyH$^+$) and 1453 cm$^{-1}$ (PyL) were considered for quantification of Brønsted ($B$) and Lewis acid sites ($L$). For calculations, the integrated molar extinction coefficients $\varepsilon_B = 1.67$ cm·µmol$^{-1}$ and $\varepsilon_L = 2.22$ cm µmol$^{-1}$ were used [52].

# 3 Results and Discussion

## 3.1 Catalyst Screening

First, a catalyst screening has been carried out employing a series of K10 catalysts. As intercalation of various ions into the material is possible, catalysts of this type offer versatile properties while being cheap and eco-friendly [37, 38]. Using the techniques described above, 5 g of treated material have been prepared for each modification method. The catalysis experiments have been carried out in batch mode and the corresponding results are depicted in Fig. 4.

The K10 catalysts exhibit a trend of decreasing selectivity to $OME_{1-6}$ with increasing TRI conversion. In consequence, selectivity to MeFo increases inversely. All catalyst treatment procedures lead to an increase in catalytic activity with the highest conversion for K10 Sn. Activity of tin exchanged montmorillonite for OME synthesis from $OME_1$ and TRI has been investigated in a study of Baranowski et al. [39]. The study concludes that intercalation of tin into the clay catalyst leads to formation of $SnO_2$ nanocrystals, increasing the accessible surface area as well as number and strength of acid sites, thus increasing catalytic activity. A slightly lower conversion with considerably higher selectivity to $OME_{1-6}$ can be observed for the acid-treated K10 H catalyst. Previous studies regarding acid-treated montmorillonite clay catalysts indicate that acid treatment leads to a decrease in total number but increase in strength of acid sites. Simultaneously, surface area and pore diameters increase, resulting in better accessibility of the acid sites. Additionally, the number of Lewis acid sites decreases while the amount of Brønsted acid sites increases, altering the nature of acidity [53]. This is important for OME synthesis in general, as literature studies show that Lewis acid sites are only active in the presence of Brønsted acid sites, indicating synergistic effects [54, 55]. Regarding the lower OME

selectivity of the K10 Sn catalyst, formation of strong Lewis acid sites by incorporation of $SnO_2$ nanocrystals is suggested [39]. In consequence, this might cause an increase in TRI decomposition without increasing OME formation. Since TRI decomposition as well as subsequent OME formation are catalyzed by acids, it is important that the reactions proceed in a concerted manner. If TRI decomposes significantly faster than OME are formed, FA accumulates, leading to increased MeFo formation. The TRI conversions are within a range of 12–36 % and selectivities to $OME_{1-6}$ are in a range of 80–96 %. While the high selectivities to OME are a very promising feature of this type of catalyst, the TRI conversion is unsatisfying.

To improve also conversion, the catalyst screening has been extended and the silico-alumino-phosphate SAPO-34 as well as the zeolites ZSM-22 and ZSM-23 have been investigated but showed no catalytic activity. In a study of Wu et al., SAPO-34 has been unsuccessfully employed for OME synthesis from DMM and TRI. This has been attributed to a molecular size of more than 4 Å for TRI, impeding access to the pore channels due to steric hindrance [43]. In the case of ZSM-22 and ZSM-23, small pore diameters of about 4.5 Å might be the reason for the lack of catalytic activity. In the next step, a series of zeolites with BEA, MFI and FAU frameworks has been investigated and showed remarkable activity, at least in part (Fig. 5).

Y zeolites generally exhibit higher selctivities but lower conversion compared to the previously described catalyst BEA-25 [27]. ZSM-5 catalysts on the other hand are more active in terms of conversion and show increased selectivity to OME in case of medium $SiO_2/Al_2O_3$ ratios. For all framework types a general trend of higher selectivity to $OME_{1-6}$ and lower TRI conversion could be observed with increasing $SiO_2/Al_2O_3$ ratios of the catalyst with exception of Y-5.2 and Y-80. These effects can be explained with the strong dependency of the catalytic activity on the acidity of the catalyst, as the number of total acid sites decreases with an increasing $SiO_2/Al_2O_3$ ratio [41]. As the nature of the acid sites changes with variation of the $SiO_2/Al_2O_3$ ratio as well, similar effects as in the case of the K10 catalysts occur. If TRI decomposes faster than OME synthesis proceeds, FA accumulates and MeFo selectivity increases. This seems to be the case especially for zeolites with low $SiO_2/Al_2O_3$ ratios, significantly reducing the OME selectivity of the process. Within the chosen reaction conditions, the reference catalyst BEA-25 exhibits a conversion of about 33 % and a total selectivity to $OME_{1-6}$ of 70 %. Zeolite Y generally exhibits higher OME selectivities but lower TRI conversion. The most suitable catalyst of this type is Y-12 with 33 % TRI conversion and an $OME_{1-6}$ selectiv-
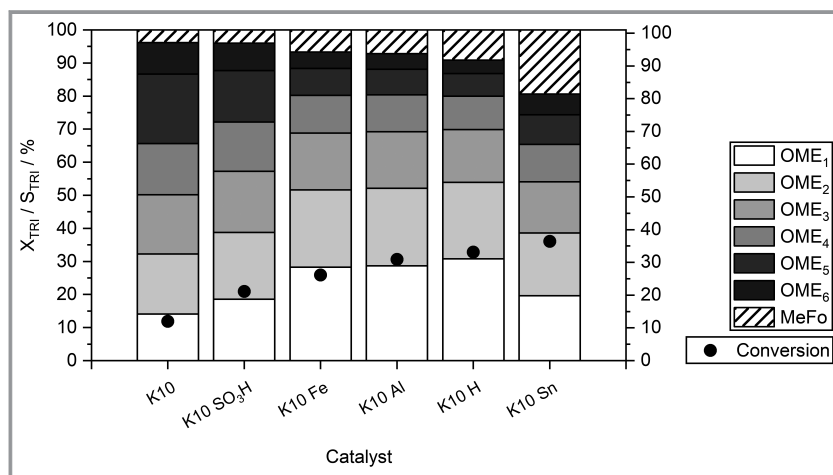
**Figure 4.** Results of batch experiments employing various K10 catalysts. TRI conversion as black symbols, selectivity to product species as pillared columns (reaction conditions: $T = 80\,°C$, $t = 6\,h$, 2.6 wt %$_R$ catalyst, $m_{total} = 40\,g$, $p = 12\,bar$, Feed 0).

www.cit-journal.com

© 2022 The Authors. Chemie Ingenieur Technik published by Wiley-VCH GmbH

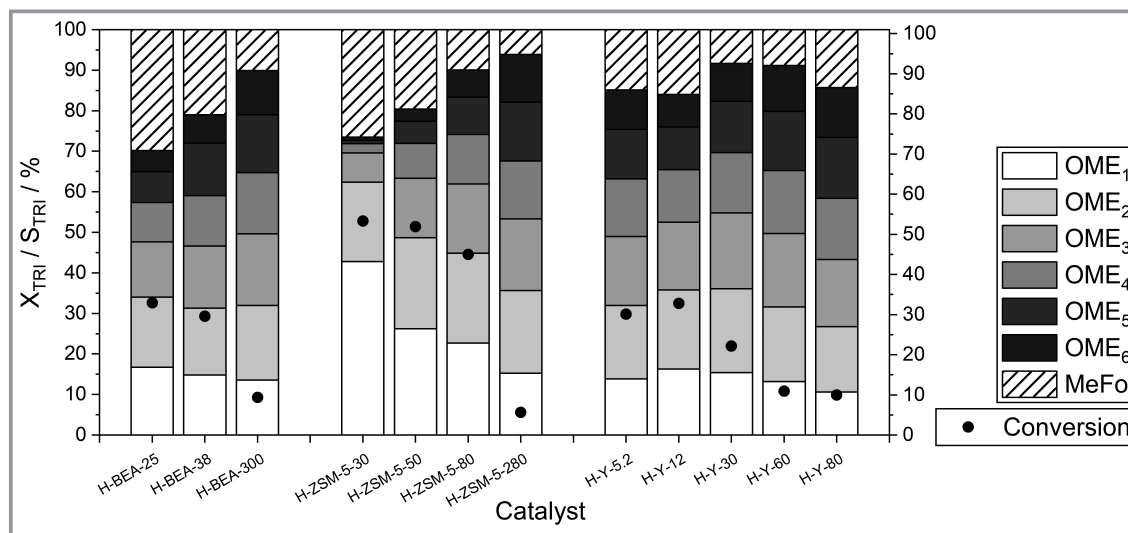*Chem. Ing. Tech.* **2022**, 94, No. 3, 1–12

**Figure 5.** Results of batch experiments employing various zeolite powders. TRI conversion as black symbols, selectivity to product species as pillared columns (reaction conditions: $T = 80\,°C$, $t = 6\,h$, $2.6\,wt\%_R$ catalyst, $m_{total} = 40\,g$, $p = 12\,bar$, Feed 0).

ity of 84 %. The most suitable catalyst for OME synthesis in this study is ZSM-5-80 with 90 % $OME_{1-6}$ selectivity and a TRI conversion of 45 %. As TRI conversion and OME selectivity are significantly higher than for other catalysts this indicates a high capability to catalyze OME formation, avoiding FA accumulation and therefore MeFo formation.

## 3.2 Continuous OME Synthesis

Due to their promising performance, the zeolites H-BEA-25 and H-ZSM-5-80 have been chosen for the continuous experiments. Extrudates of these zeolites have been employed and structural characteristics have been determined which are listed in Tab. 3. Surface areas of both catalysts are, as expected, considerably lower compared to the powders, which is due to the shaping process. Notably, H-BEA-25 exhibits significantly higher values for the surface area as well as pore volume than H-ZSM-5-80. While the acid site concentration is considerable higher as well, the nature of acidity in matters of the ratio of Brønsted to Lewis ($B/L$) acid sites differs. As the nature of acidity is decisive for OME formation due to the synergistic effects this is an important difference between the two catalysts.

To compare the activity of the catalysts and to study the influence of residence time on product spectra, a broad $WHSV$ range from 5 to $75\,h^{-1}$ has been investigated. The results of the experiments with H-BEA-25 and H-ZSM-5-80 employing Feed 1 are depicted in Fig. 6.

Comparing the results of the continuous experiments to the batch experiments, values for selectivity to $OME_{1-6}$ and TRI conversion change considerably. This can be attributed to the higher reaction temperature, which increases reaction rates and favors MeFo formation, thus reducing values for selectivity to $OME_{1-6}$ and increasing TRI conversion. Upon increasing the $WHSV$, the conversion of TRI decreases from 95 to 42 % while the selectivity to $OME_{1-6}$ increases from 24.2 to 51.5 % (Fig. 6a). This corresponds to an optimum yield of $OME_{1-6}$ of about 31 % at a $WHSV$ of $62.5\,h^{-1}$. Additionally, the $ACL$ increases, indicating larger fractions of higher OME molecules and demonstrating the potential of kinetic control to maximize the yield of higher OME oligomers for fuel applications. With respect to the reaction mechanism this indicates that a large portion of OME is formed by direct incorporation of TRI in DME (Eq. (3)). Such a direct incorporation has been described in a theoretical study of Goncalves et al. addressing the reaction of DMM with TRI and revealing that this reaction path is more favorable

**Table 3.** Structural characteristics of zeolite extrudates for continuous OME synthesis.

| Catalyst | Trade name | Surface area [$m^2g^{-1}$] | | | Pore volume [$cm^3g^{-1}$] | | Acidity [$mmol\,g^{-1}$] | | |
|---|---|---|---|---|---|---|---|---|---|
| | | BET | micro[a] | external[a] | micro[a] | meso[b] | $c_B$[c] | $c_L$[d] | $B/L$ |
| H-BEA-25 | CP814E*CY | 574 | 335 | 240 | 0.138 | 0.665 | 0.47 | 0.41 | 1.14 |
| H-ZSM-5-80 | CBV8014CY | 383 | 267 | 116 | 0.115 | 0.266 | 0.29 | 0.15 | 1.91 |

a) Based on the t-plot method; b) based on the Barret-Joyner-Halenda (BJH) method using the desorption branch; c) $1543\,cm^{-1}$, $T_{des} = 250\,°C$; d) $1453\,cm^{-1}$, $T_{des} = 250\,°C$.
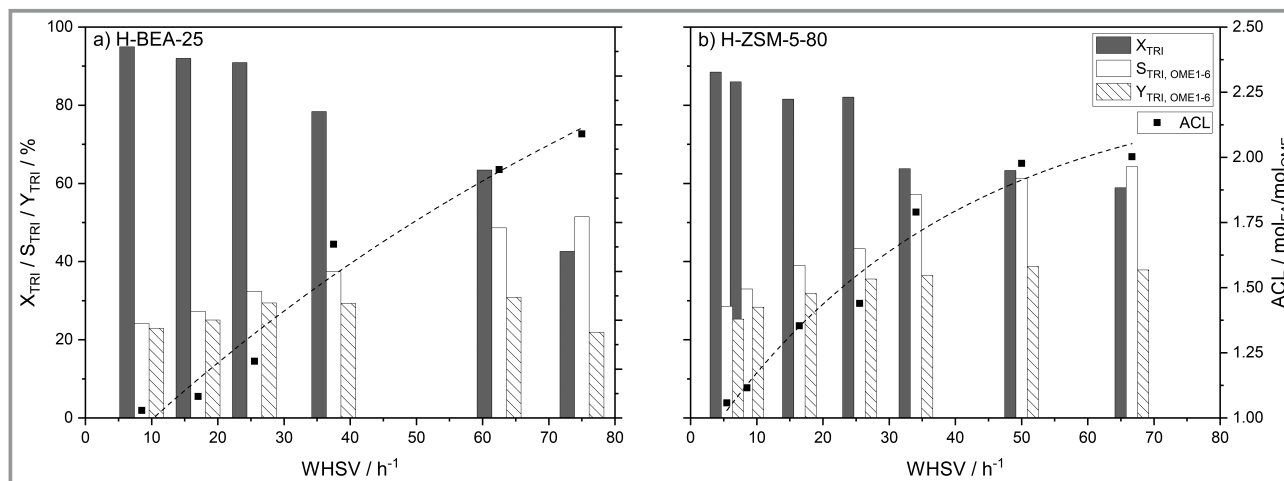
**Figure 6.** Results of continuous OME synthesis employing (a) H-BEA-25 and (b) H-ZSM-5-80 extrudates as catalysts. TRI conversion, selectivity and yield of $OME_{1-6}$ as columns, average chain lengths (ACL) as black symbols (reaction conditions: $T = 100\,°C$, $\dot{m}_{reactant} = 2–8\,g\,min^{-1}$, $p = 60\,bar$, Feed 1).

compared to initial TRI decomposition (Eq. (1) and (2)) [56, 57]. This leads to initially high shares of $OME_3$, which will subsequently react to smaller OME molecules via transacetalization (Eq. (5)), converging the equilibrium distribution. In the case of high *WHSV* values the system will not reach equilibrium, resulting in higher *ACL* values.

The corresponding experiments employing H-ZSM-5-80 and using the same feed composition and *WHSV* range are illustrated in Fig. 6b. Similar trends for conversion and selectivity as for H-BEA-25 can be observed. The selectivity to $OME_{1-6}$ is significantly higher than in the experiments with H-BEA-25, which is in accordance with the batch experiments. It is noteworthy that the TRI conversion is lower than in the experiments with H-BEA-25, which is in contrast to the batch experiments. This can be attributed to the strong formation of MeFo for H-BEA-25 at temperatures exceeding 90 °C [27], resulting in a high TRI conversion. As MeFo formation is significantly less pronounced for H-ZSM-5-80, values for TRI conversion remain lower. However, the conversion decreases significantly less upon increasing the *WHSV* and remains at high values. At a *WHSV* of $66\,h^{-1}$ the conversion amounts to 59 %, resulting in permanently high yields of $OME_{1-6}$. The highest yield of about 39 % was obtained at a *WHSV* of $50\,h^{-1}$, emphasizing the suitability of H-ZSM-5-80 to catalyze OME synthesis from DME and TRI. As surface area, pore volume and the concentration of acid sites is lower than for the BEA catalyst, this illustrates the strong influence of the nature of acid sites for OME synthesis. H-ZSM-5-80 exhibits Brønsted and Lewis acid sites in a ratio of 1.91 in contrast to 1.14 for H-BEA-25, showing the synergism between both types of acid sites, which has also been observed within other studies on OME synthesis [43, 54, 55].

To further improve the OME synthesis process, dilution with dodecane was reduced to 10 wt % (Feed 2) in another set of continuous experiments (Fig. 7a). Confirming the

results of the previous experiments, similar trends can be observed. However, conversion and selectivity are significantly increased. At low *WHSV* total conversion can be reached and even at a *WHSV* of $68.5\,h^{-1}$ conversion remains at a high level, amounting to 57.5 %. Selectivity to $OME_{1-6}$ is in the range from 35 to 73 % for all operating points. The yield of $OME_{1-6}$ exhibits a maximum of about 48 % at *WHSV* values of 34 and $51\,h^{-1}$. Due to the higher conversion and a higher *ACL* value of 2.0 the operating point at $51\,h^{-1}$ seems to be the most suitable for the synthesis of OME fuels. The product spectrum and mass fraction of the compounds in the product stream are depicted in Fig. 7b. The total mass of products amounts to 30.68 % of the product stream, with 24.52 % $OME_{1-6}$. The $OME_{3-5}$ fraction of the oligomers composing the fraction relevant for fuel applications adds up to 8.65 % of the product stream, demonstrating the potential of this pathway. While not converted reactants and OME fractions not relevant for fuel applications can simply be recycled, MeFo needs to be separated from the product stream. As the boiling point of MeFo is lower than that of $OME_1$ this might be achieved by a preceding distillation step. However, synthesis and purification of OME mixtures are a subject of ongoing research and experimental studies regarding downstream processes have to be carried out yet. As MeFo is currently investigated as a gasoline substitute, combined production of both types of fuel in a single process with adaptable selectivity becomes feasible.

## 4 Conclusion

Various catalysts have been tested for OME synthesis from DME and TRI. The reactions have been carried out batchwise in liquid phase. Suitability of K10 clay catalysts has been demonstrated and ion exchange procedures have been
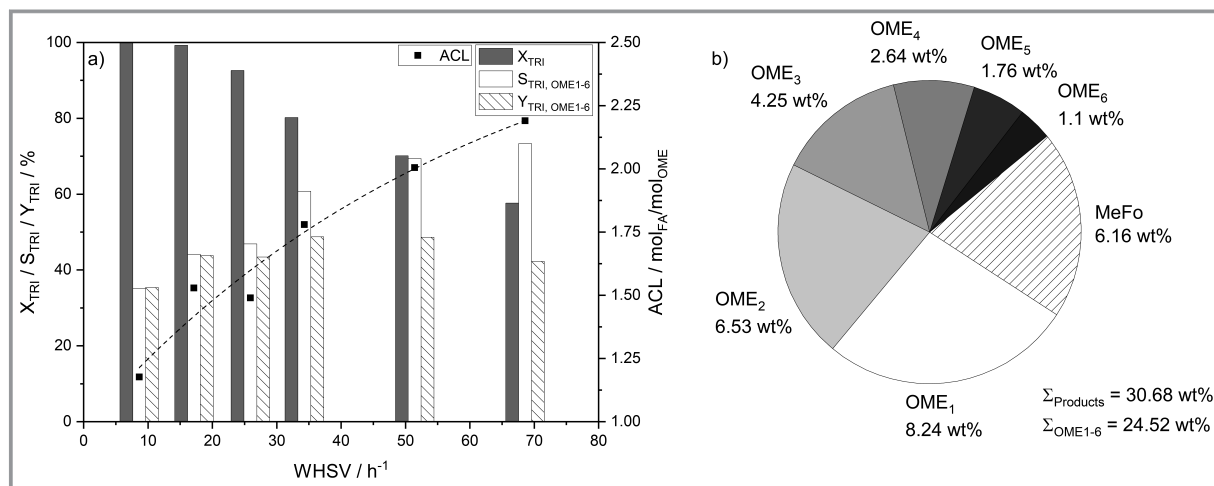
www.cit-journal.com

© 2022 The Authors. Chemie Ingenieur Technik published by Wiley-VCH GmbH

*Chem. Ing. Tech.* **2022**, *94*, No. 3, 1–12

**Figure 7.** Results of continuous OME synthesis employing H-ZSM-5-80 extrudates. (a) TRI conversion, selectivity and yield of $OME_{1-6}$ as columns, average chain lengths ($ACL$) as black symbols (reaction conditions: 100 °C, Zeolite H-ZSM-5-80, $\dot{m}_{reactant}$ = 2–8 g min$^{-1}$, $p$ = 60 bar, Feed 2). (b) Product distribution at a $WHSV$ of 51 h$^{-1}$, values related to the mass fraction of the respective compound in the product stream.

used to further improve catalytic activity. Furthermore, zeolites BEA, ZSM-5 and Y have been identified as highly active catalysts and the influence of $SiO_2/Al_2O_3$ ratio has been investigated systematically. Among the employed catalysts, H-ZSM-5-80 has shown the most advantageous properties regarding OME synthesis. The catalyst exhibits high conversion and selectivity to OME, which results in overall high yields. Furthermore, the findings of this study confirm the advantages of an anhydrous OME synthesis process as besides MeFo, which is an interesting substitute for gasoline, no significant side product formation has been observed. Furthermore, as this catalyst is widely used in petrochemical industry, it is available in the large quantities necessary for the production of synthetic fuel.

Additionally, OME synthesis from DME has been demonstrated successfully in a continuously operating laboratory setup employing H-BEA-25 as well as H-ZSM-5-80 extrudates as catalysts. By variation of the $WHSV$, kinetic control of the product spectrum has been used to optimize the $ACL$ and therefore the yield of $OME_{3-5}$. Furthermore, conclusions with respect to the reaction mechanism can be drawn from this effect. Increasing $ACL$ values with increasing $WHSV$ indicate initial formation of OME by direct incorporation of TRI in DME, validating theoretical investigations from previous studies. Regarding the influence of acidity on OME synthesis, synergistic effects between Brønsted and Lewis acid sites could be observed. At a WHSV value of 51 h$^{-1}$ 70 % conversion of TRI with 69 % selectivity to OME could be reached, resulting in a yield of about 48 %. This resulted in a mass fraction of $OME_{3-5}$ of 8.65 wt % in the product stream in a single reactor pass employing H-ZSM-5-80, which emphasizes the high potential of this production pathway.

Future work regarding this promising OME production pathway aims for optimizing the continuous synthesis process. Separation of OME product mixtures is subject of ongoing investigations on aqueous OME synthesis and should be extended to OME synthesis from DME to evaluate the potential for industrial application. By modification of the experimental setup used in this study a wider range of operating points can become accessible. This allows for optimization of the process conditions concerning $WHSV$, temperature and reactant mixtures as well as long-term studies to investigate the stability of the catalyst. These activities will be supplemented by employing other formaldehyde sources and thus, a broad data base for process scale-up will become available.

## Supporting Information

Supporting Information for this article can be found under DOI: https://doi.org/10.1002/cite.202100173.

## Symbols used

| | | |
|---|---|---|
| $A$ | [m$^2$g$^{-1}$] | specific surface area |
| $ACL$ | [mol$_{FA}$mol$_{OME}^{-1}$] | average chain length |
| $c$ | [mmol g$^{-1}$] | concentration |

| $L$ | [–] | Lewis |
|---|---|---|
| $M$ | [g mol$^{-1}$] | molar mass |
| $m$ | [g] | mass |
| $\dot{m}$ | [g min$^{-1}$] | mass flow |
| $n$ | [mol] | amount of substance |
| $p$ | [bar] | pressure |
| $q$ | [–] | number of protons related to the signal |
| $RF$ | [–] | response factor |
| $S$ | [%] | selectivity |
| $V$ | [cm$^3$g$^{-1}$] | specific volume |
| $X$ | [%] | conversion |
| $Y$ | [%] | yield |
| $WHSV$ | [h$^{-1}$] | weight hourly space velocity |
| $\omega$ | [wt %] | weight fraction |

## Sub- and Superscripts

| $0$ | reference |
|---|---|
| $B$ | Brønsted |
| $L$ | Lewis |
| $R$ | related to the reactants |

## Abbreviations

| DME | dimethyl ether |
|---|---|
| FA | formaldehyde |
| MeFo | methyl formate |
| OME | oxymethylene ether |
| TRI | trioxane |

## References

[1] K. Hackbarth, P. Haltenort, U. Arnold, J. Sauer, *Chem. Ing. Tech.* **2018**, *90 (10)*, 1520–1528. DOI: https://doi.org/10.1002/cite.201800068

[2] D. Deutsch, D. Oestreich, L. Lautenschütz, P. Haltenort, U. Arnold, J. Sauer, *Chem. Ing. Tech.* **2017**, *89 (4)*, 486–489. DOI: https://doi.org/10.1002/cite.201600158

[3] L. Lautenschütz, D. Oestreich, P. Seidenspinner, U. Arnold, E. Dinjus, J. Sauer, *Fuel* **2016**, *173*, 129–137. DOI: https://doi.org/10.1016/j.fuel.2016.01.060

[4] H. Liu, X. Ma, B. Li, L. Chen, Z. Wang, J. Wang, *Fuel* **2017**, *209*, 62–68. DOI: https://doi.org/10.1016/j.fuel.2017.07.066

[5] J. V. Pastor, A. García, C. Micó, F. Lewiski, *Appl. Energy* **2020**, *260*, 114238. DOI: https://doi.org/10.1016/j.apenergy.2019.114238

[6] P. Dworschak, V. Berger, M. Härtl, G. Wachtmeister, *SAE Tech. Pap. Ser.* **2020**, *2020-01-0805*. DOI: https://doi.org/10.4271/2020-01-0805

[7] M. Härtl, P. Seidenspinner, E. Jacob, G. Wachtmeister, *Fuel* **2015**, *153*, 328–335. DOI: https://doi.org/10.1016/j.fuel.2015.03.012

[8] M. Härtl, P. Seidenspinner, G. Wachtmeister, E. Jacob, *MTZ Motortech. Z.* **2014**, *75 (7)*, 68–73. DOI: https://doi.org/10.1007/s35146-014-0392-7

[9] H. Liu, Z. Wang, J. Wang, X. He, Y. Zheng, Q. Tang, J. Wang, *Energy* **2015**, *88*, 793–800. DOI: https://doi.org/10.1016/j.energy.2015.05.088

[10] A. García, A. Gil, J. Monsalve-Serrano, R. Lago Sari, *Fuel* **2020**, *275*, 117898. DOI: https://doi.org/10.1016/j.fuel.2020.117898

[11] D. Pélerin, K. Gaukel, M. Härtl, E. Jacob, G. Wachtmeister, *Fuel* **2020**, *259*, 116231. DOI: https://doi.org/10.1016/j.fuel.2019.116231

[12] Z. Wang, H. Liu, J. Zhang, J. Wang, S. Shuai, *Energy Procedia* **2015**, *75*, 2337–2344. DOI: https://doi.org/10.1016/j.egypro.2015.07.479

[13] J. Liu, P. Sun, H. Huang, J. Meng, X. Yao, *Appl. Energy* **2017**, *202*, 527–536. DOI: https://doi.org/10.1016/j.apenergy.2017.05.166

[14] D. Oestreich, L. Lautenschütz, U. Arnold, J. Sauer, *Fuel* **2018**, *214*, 39–44. DOI: https://doi.org/10.1016/j.fuel.2017.10.116

[15] X. Zhang, A. O. Oyedun, A. Kumar, D. Oestreich, U. Arnold, J. Sauer, *Biomass Bioenergy* **2016**, *90*, 7–14. DOI: https://doi.org/10.1016/j.biombioe.2016.03.032

[16] A. O. Oyedun, A. Kumar, D. Oestreich, U. Arnold, J. Sauer, *Biofuels, Bioprod. Biorefin.* **2018**, *12 (4)*, 694–710. DOI: https://doi.org/10.1002/bbb.1887

[17] C. Hank, L. Lazar, F. Mantei, M. Ouda, R. J. White, T. Smolinka, A. Schaadt, C. Hebling, H.-M. Henning, *Sustainable Energy Fuels* **2019**, *3 (11)*, 3219–3233. DOI: https://doi.org/10.1039/c9se00658c

[18] S. Deutz, D. Bongartz, B. Heuser, A. Kätelhön, L. Schulze Langenhorst, A. Omari, M. Walters, J. Klankermayer, W. Leitner, A. Mitsos, S. Pischinger, A. Bardow, *Energy Environ. Sci.* **2018**, *11 (2)*, 331–343. DOI: https://doi.org/10.1039/C7EE01657C

[19] N. Mahbub, A. O. Oyedun, A. Kumar, D. Oestreich, U. Arnold, J. Sauer, *J. Cleaner Prod.* **2017**, *165*, 1249–1262. DOI: https://doi.org/10.1016/j.jclepro.2017.07.178

[20] J. Voggenreiter, J. Burger, *Ind. Eng. Chem. Res.* **2021**, *60 (6)*, 2418–2429. DOI: https://doi.org/10.1021/acs.iecr.0c05780

[21] C. J. Baranowski, A. M. Bahmanpour, O. Kröcher, *Appl. Catal., B* **2017**, *217*, 407–420. DOI: https://doi.org/10.1016/j.apcatb.2017.06.007

[22] D. Oestreich, L. Lautenschütz, U. Arnold, J. Sauer, *Chem. Eng. Sci.* **2017**, *163*, 92–104. DOI: https://doi.org/10.1016/j.ces.2016.12.037

[23] N. Schmitz, E. Ströfer, J. Burger, H. Hasse, *Ind. Eng. Chem. Res.* **2017**, *56 (40)*, 11519–11530. DOI: https://doi.org/10.1021/acs.iecr.7b02314

[24] N. Schmitz, F. Homberg, J. Berje, J. Burger, H. Hasse, *Ind. Eng. Chem. Res.* **2015**, *54 (25)*, 6409–6417. DOI: https://doi.org/10.1021/acs.iecr.5b01148

[25] N. Schmitz, J. Burger, H. Hasse, *Ind. Eng. Chem. Res.* **2015**, *54 (50)*, 12553–12560. DOI: https://doi.org/10.1021/acs.iecr.5b04046

[26] C. F. Breitkreuz, N. Schmitz, E. Ströfer, J. Burger, H. Hasse, *Chem. Ing. Tech.* **2018**, *90 (10)*, 1489–1496. DOI: https://doi.org/10.1002/cite.201800038

[27] P. Haltenort, K. Hackbarth, D. Oestreich, L. Lautenschütz, U. Arnold, J. Sauer, *Catal. Commun.* **2018**, *109*, 80–84. DOI: https://doi.org/10.1016/j.catcom.2018.02.013

[28] R. Peláez, P. Marín, S. Ordóñez, *Chem. Eng. J.* **2020**, *396*, 125305. DOI: https://doi.org/10.1016/j.cej.2020.125305

[29] P. Haltenort, L. Lautenschütz, U. Arnold, J. Sauer, *Top. Catal.* **2019**, *62 (5–6)*, 551–559. DOI: https://doi.org/10.1007/s11244-019-01188-9

[30] Y. Zhao, Z. Xu, H. Chen, Y. Fu, J. Shen, *J. Energy Chem.* **2013**, *22 (6)*, 833–836. DOI: https://doi.org/10.1016/S2095-4956(14)60261-8

[31] L. Lautenschütz, D. Oestreich, P. Haltenort, U. Arnold, E. Dinjus, J. Sauer, *Fuel Process. Technol.* **2017**, *165*, 27–33. DOI: https://doi.org/10.1016/j.fuproc.2017.05.005

[32] A. Peter, S. M. Fehr, V. Dybbert, D. Himmel, I. Lindner, E. Jacob, M. Ouda, A. Schaadt, R. J. White, H. Scherer, I. Krossing, *Angew. Chem., Int. Ed.* **2018**, *57 (30)*, 9461–9464. DOI: https://doi.org/10.1002/anie.201802247

[33] T. Maier, M. Härtl, E. Jacob, G. Wachtmeister, *Fuel* **2019**, *256*, 115925. DOI: https://doi.org/10.1016/j.fuel.2019.115925

[34] S. Blochum, B. Gadomski, M. Retzlaff, F. Thamm, C. Kraus, M. Härtl, R. Gelhausen, S. Hoppe, G. Wachtmeister, *SAE Tech. Pap. Ser.* **2021**, *2021-01-0561*. DOI: https://doi.org/10.4271/2021-01-0561

[35] K. A. Bernard, J. D. Atwood, *Organometallics* **1988**, *7 (1)*, 235–236. DOI: https://doi.org/10.1021/om00091a037

[36] C. J. Baranowski, T. Fovanna, M. Roger, M. Signorile, J. McCaig, A. M. Bahmanpour, D. Ferri, O. Kröcher, *ACS Catal.* **2020**, *10 (15)*, 8106–8119. DOI: https://doi.org/10.1021/acscatal.0c01805

[37] A. Vaccari, *Appl. Clay Sci.* **1999**, *14 (4)*, 161–198. DOI: https://doi.org/10.1016/S0169-1317(98)00058-1

[38] A. M. Bahmanpour, F. Héroguel, C. J. Baranowski, J. S. Luterbacher, O. Kröcher, *Appl. Catal., A* **2018**, *560*, 165–170. DOI: https://doi.org/10.1016/j.apcata.2018.05.006

[39] C. J. Baranowski, A. M. Bahmanpour, F. Héroguel, J. S. Luterbacher, O. Kröcher, *ChemCatChem* **2019**, *11 (13)*, 3010–3021. DOI: https://doi.org/10.1002/cctc.201900502

[40] A. Deshmukh, V. K. Gumaste, B. M. Bhawal, *Synth. Commun.* **1995**, *25 (24)*, 3939–3944. DOI: https://doi.org/10.1080/00397919508011470

[41] A. Fink, C. H. Gierlich, I. Delidovich, R. Palkovits, *ChemCatChem* **2020**, *12 (22)*, 5710–5719. DOI: https://doi.org/10.1002/cctc.202000972

[42] A. Grünert, P. Losch, C. Ochoa-Hernández, W. Schmidt, F. Schüth, *Green Chem.* **2018**, *20 (20)*, 4719–4728. DOI: https://doi.org/10.1039/C8GC02617C

[43] J. Wu, S. Wang, H. Li, Y. Zhang, R. Shi, Y. Zhao, *Nanomaterials* **2019**, *9 (9)*, 1192. DOI: https://doi.org/10.3390/nano9091192

[44] C. J. Baranowski, A. M. Bahmanpour, F. Héroguel, J. S. Luterbacher, O. Kröcher, *Catal. Sci. Technol.* **2019**, *9 (2)*, 366–376. DOI: https://doi.org/10.1039/C8CY02194E

[45] J. Wu, H. Zhu, Z. Wu, Z. Qin, L. Yan, B. Du, W. Fan, J. Wang, *Green Chem.* **2015**, *17 (4)*, 2353–2357. DOI: https://doi.org/10.1039/C4GC02510E

[46] J. M. Adams, *Clays Clay Miner.* **1983**, *31 (2)*, 129–136. DOI: https://doi.org/10.1346/CCMN.1983.0310207

[47] C. Ravindra Reddy, G. Nagendrappa, B. S. Jai Prakash, *Catal. Commun.* **2007**, *8 (3)*, 241–246. DOI: https://doi.org/10.1016/j.catcom.2006.06.023

[48] C. R. Reddy, B. Vijayakumar, P. Iyengar, G. Nagendrappa, B. S. Jai Prakash, *J. Mol. Catal. A: Chem.* **2004**, *223 (1–2)*, 117–122. DOI: https://doi.org/10.1016/j.molcata.2003.11.039

[49] F. Shirini, A. F. Shojaei, S. Z. D. Heirati, *Phosphorus, Sulfur Silicon Relat. Elem.* **2016**, *191 (6)*, 944–951. DOI: https://doi.org/10.1080/10426507.2015.1119141

[50] M. Ouda, G. Yarce, R. J. White, M. Hadrich, D. Himmel, A. Schaadt, H. Klein, E. Jacob, I. Krossing, *React. Chem. Eng.* **2017**, *2 (1)*, 50–59. DOI: https://doi.org/10.1039/C6RE00145A

[51] C. Baerlocher, L. B. McCusker, D. H. Olson, *Atlas of zeolite framework types*, 6th ed., Elsevier, Amsterdam **2007**.

[52] C. A. Emeis, *J. Catal.* **1993**, *141 (2)*, 347–354. DOI: https://doi.org/10.1006/jcat.1993.1145

[53] U. Flessner, D. Jones, J. Rozière, J. Zajac, L. Storaro, M. Lenarda, M. Pavan, A. Jiménez-López, E. Rodríguez-Castellón, M. Trombetta, G. Busca, *J. Mol. Catal. A: Chem.* **2001**, *168 (1–2)*, 247–256. DOI: https://doi.org/10.1016/S1381-1169(00)00540-9

[54] F. Liu, T. Wang, Y. Zheng, J. Wang, *J. Catal.* **2017**, *355*, 17–25. DOI: https://doi.org/10.1016/j.jcat.2017.08.014

[55] C. J. Baranowski, M. Roger, A. M. Bahmanpour, O. Kröcher, *ChemSusChem* **2019**, *12 (19)*, 4421–4431. DOI: https://doi.org/10.1002/cssc.201901814

[56] T. J. Goncalves, U. Arnold, P. N. Plessow, F. Studt, *ACS Catal.* **2017**, *7 (5)*, 3615–3621. DOI: https://doi.org/10.1021/acscatal.7b00701

[57] T. J. Goncalves, P. N. Plessow, F. Studt, *ChemCatChem* **2019**, *11 (7)*, 1949–1954. DOI: https://doi.org/10.1002/cctc.201900115

# Continuous Synthesis of Oxymethylene Ether Fuels from Dimethyl Ether in a Heterogeneously Catalyzed Liquid Phase Process

*Marius Drexler, Philipp Haltenort, Ulrich Arnold\*, Jörg Sauer*

**Research Article:** In the context of alternative diesel fuels, this study addresses the synthesis of oxymethylene ethers from dimethyl ether and trioxane. A series of catalysts has been tested and continuous production could be demonstrated. The experimental results provide insights into structure performance relationships of the catalysts as well as the reaction mechanism. ⋯⋯⋯⋯⋯⋯⋯⋯⋯⋯⋯⋯⋯⋯⋯⋯⋯⋯⋯⋯⋯⋯⋯⋯⋯⋯⋯⋯⋯⋯⋯⋯⋯ ■

Supporting Information
available online